

Numerical and physical simulation of new SPD method combining extrusion and equal channel angular pressing for AZ31 magnesium alloy

ZHANG Ding-fei(张丁非)^{1,2}, HU Hong-jun(胡红军)^{1,3}, PAN Fu-sheng(潘复生)^{1,2},
YANG Ming-bo(杨明波)³, ZHANG Jun-ping(张钧萍)²

1. National Engineering Research Center for Magnesium Alloys, Chongqing University, Chongqing 400044, China;
2. College of Materials Science and Engineering, Chongqing University, Chongqing 400045, China;
3. College of Materials Science and Engineering, Chongqing University of Technology, Chongqing 400050, China;

Received 25 December 2008; accepted 8 June 2009

Abstract: A new severe plastic deformation (SPD) including initial forward extrusion and subsequent shearing process (ES) was proposed. The influence of the ES forming on the grain refinement of the microstructure was researched. The components of ES forming die were manufactured and installed to Gleeble1500D thermo-mechanical simulator. The microstructure observations were carried out on the as-extruded rods (as-received) and ES formed rods. From the simulation results, ES forming can increase the cumulative strain enormously and the volume fraction of dynamic recrystallization. From the physical modeling results, the microstructures can be refined.

Key words: magnesium alloy; severe plastic deformation; dynamic recrystallization; microstructures refinement

1 Introduction

As the lightest structural material of engineering significance, Mg alloys have attracted considerable attention recently[1–2]. However, Mg alloys exhibit poor formability and possess only moderate strength compared with Al alloys. One of the promising methods for increasing ductility and strength of Mg alloys is microstructure refinement. A fine-grained material is harder and stronger than coarse-grained one because it has a greater total grain boundary area to impede dislocation motion[3–4].

In recent years, bulk nanostructure materials processed by severe plastic deformation (SPD), such as equal-channel angular extrusion (ECAE), have attracted the growing interest[5–14]. As the cross-section of the material remains unaltered, it can be processed over and over again to impart uniform large plastic strains. In spite of its invention in the early 1980s, the process does not progress as much as desired and is still confined to the laboratory scale. A new processing procedure[15–16]

was used to extrude a cast Mg-9%Al alloy involving the sequential application of extrusion and equal-channel angular pressing (EX-ECAP). Experiments showed that the Mg-9%Al alloy has an initial grain size of about 50 μm after casting but it was reduced to about 12 μm after extrusion and was further reduced to about 0.7 μm when the extruded alloy was subjected to ECAP for 2 passes at 473 K. Although the cast alloy exhibits extremely limited ductility and the extruded alloy was only moderately ductile, it was demonstrated that processing by EX-ECAP produces excellent superplastic ductility including the occurrence of both low-temperature superplasticity and high-strain-rate superplasticity. MATSUBARA et al[16] used the EX-ECAP to prepare the ultrafine magnesium, but the ECAP process was only used to prepare nanocrystalline material in the lab scale, and there still existed an unbridgeable gap between the experimentation and applications in industry. The EX-ECAP usually includes more than 2 steps, and the material endures intricate diversification of forming environments including processing temperature and may be oxidized.

Foundation item: Project(2007CB613700) supported by the National Basic Research Program of China; Project(2007BAG06B04) supported by the National Science and Technology Pillar Program during the 11th Five-Year Plan Period; Project(50725413) supported by the National Natural Science Foundation of China; Project(CSTC2009AB4008) supported by Chongqing Science and Technology Development Program, China

Corresponding author: ZHANG Ding-fei; Tel/Fax: +86-23-65112491; E-mail: zhangdingfei@cqu.edu.cn
DOI: 10.1016/S1003-6326(09)60165-5

In the present research, a new approach was introduced to prepare rods made of magnesium alloy, which includes two consecutive processes (initial forward extrusion and subsequent shearing process, abbreviated as ES). The geometrical and numerical models based on simulation theories were built to predict the evolution of the strain field and volume fraction of dynamic recrystallization. The components of ES forming die were manufactured and installed to Gleeble1500D thermo-mechanical simulator. Physical simulations were done by executing the computer program of simulator. The microstructures of AZ31 Mg alloy sampled from as-received and ES-formed rods were observed. The results of simulations and physical modeling were discussed and compared.

2 Theoretical basis of simulation

This study performs rigid-plastic finite element simulations using DEFORMTM-3D software (Version 5.0). This mechanism occurs during deformation when the strain exceeds a critical value, the driving force for the removal of dislocations. Experimental data must be collected under various strains, strain rates, and temperatures. The critical strain, ϵ_c , is usually a fraction of the strain ϵ_p at which the flow stress reaches its maximum (and flow softening due to dynamic crystallization):

$$\epsilon_c = \alpha_2 \epsilon_p \tag{1}$$

The value of ϵ_p is determined experimentally and is usually a function of strain rate $\dot{\epsilon}$, temperature T , and initial grain size d_0 :

$$\epsilon_p = \alpha 1 d_0^{n1} \dot{\epsilon}^{m1} \exp[Q_1/(RT)] + c1 \tag{2}$$

where ϵ_p denotes the strain corresponding to the flow stress maximum; $\alpha 1$ is the material datum; $n1$, $m1$ and $c1$ are exponents.

An Avrami equation is also used to describe the relation between DRX volume fraction and the effective strain:

$$X_{DRX} = 1 - \exp \left[-\beta_d \left(\frac{\epsilon - a_{10} \epsilon_p}{\epsilon_{0.5}} \right)^{k_d} \right] \tag{3}$$

where $\epsilon_{0.5}$ denotes the strain for 50% crystallization (Q_5 is the experimental datum and c_5 is the material datum):

$$\epsilon_{0.5} = \alpha 5 d_0^{n5} \dot{\epsilon}^{m5} \exp[Q_5/(RT)] + c_5 \tag{4}$$

The DRX grain size is expressed as

$$d_{DRX} = \alpha 8 d_0^{k8} \dot{\epsilon}^{n8} \epsilon^{m8} \exp[Q_8/(RT)] + c_8 \tag{5}$$

where Q_8 is the experimental datum; $\alpha 8$, k_8 , n_8 , m_8 and

c_8 are material data.

If $d_{DRX} > d_0$, then let $d_{DRX} = d_0$.

3 Simulation conditions

A commercial wrought alloy AZ31B (as-extruded, Mg-3%Al-1%Zn, mass fraction) was used in the simulation and extrusion experiments. The extrusion tooling consisting of die, container and ram was made of the H13 hot-work tool steel. The physical properties of AZ31B are given in Table 1. Its specific heat and thermal conductivity are dependent on temperature, with the curves shown in Fig.1 and Fig.2, respectively. The flow stress–strain data of the AZ31 alloy (as-extruded) were determined through hot compression tests using Gleeble1500D machine in Laboratory of National Engineering Research Center for Magnesium Alloys, China. By taking the effect of deformation heating during hot compression at high strain rates on the actual specimen temperature into account, the flow stress curves measured in these tests were corrected and a set of flow stress—strain curves as examples are shown in Fig.3. The data over a temperature range of 250–450 °C and a strain rate range of 0.005–5 s⁻¹ were input into the material property module of the DEFORMTM-3D software.

The whole ES forming was simulated by means of the DEFORM-3D code and the coefficients of the dynamic crystallization equations were obtained by the

Table 1 Physical properties of AZ31B workpiece

Property	Value
Poisson ratio	0.35
Coefficient of linear expansion/K ⁻¹	26.8 × 10 ⁻⁵
Density/(kg·m ⁻³)	1 780
Elastic modulus/MPa	45 000
Emissivity	0.12

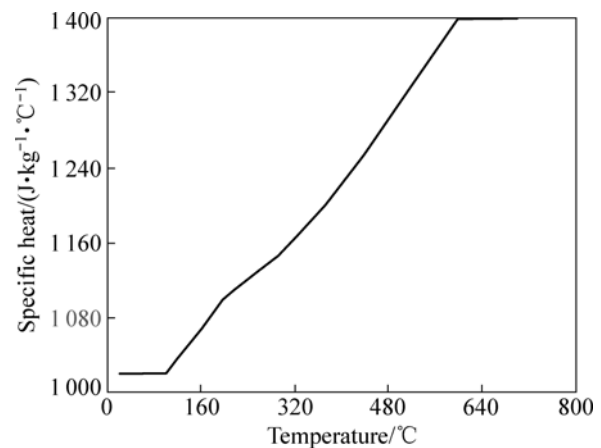


Fig.1 Curve of specific heat with temperature for AZ31 magnesium alloy

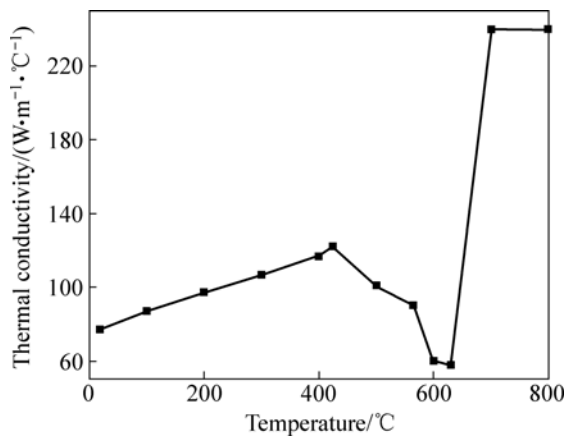


Fig.2 Curve of thermal conductivity with temperature for AZ31 magnesium alloy

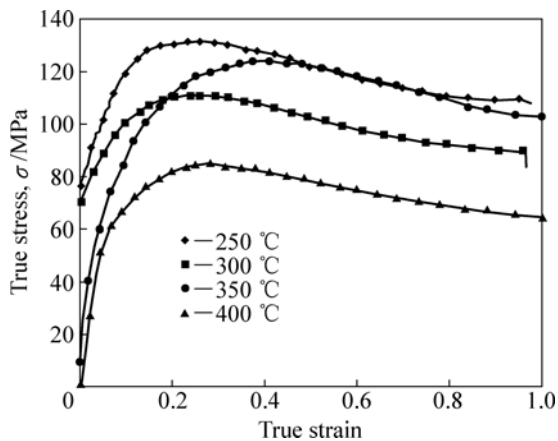


Fig.3 True stress — true strain curves of AZ31 alloy (as-extruded) obtained from compression tests at different strain rates and temperatures

comparison with the experimental compression results. The coefficients of the equations of dynamic recrystallization for Eqs.(1)–(5) are listed in Table 2. The finite element method (FEM) models for numerical simulation including extrusion ram, billet and ES die are illustrated in Fig.4. Simulation and experimental parameters including geometry and process parameters are listed in Table 3, and the FEM element numbers and meshing methods are numerated. The process parameters (initial temperature, friction factor, etc.) are regarded as boundary and initial conditions of simulation in DEFORMTM-3D software.

Table 2 Coefficients of equations of dynamic recrystallization

α_1	n_1	m_1	Q_1	c_1	α_5
2.6e-05	0	0.31	42 820	0	0.1336
n_5	m_5	Q_5	k_d	α_8	n_8
0	0.0406	5 608.078	1.06	173.83	0
m_8	Q_8	c_8	c_5	β_d	
-0.1	-13 813	0	0	0.209	

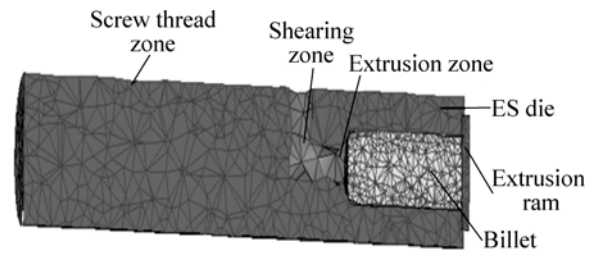


Fig.4 Die structure and FEM model of ES forming

Table 3 Simulation and experimental parameters including geometry and process conditions

Parameter	Value
Billet length/mm	10
Billet diameter(as-extruded)/mm	5.6
Insider diameter of container/mm	6
Outside diameter of container/mm	20
Die bearing length/mm	5
Extrusion ratio	4
Initial billet temperature/°C	350
Initial tooling temperature/°C	350
Temperature range for flow stress measurement/°C	250–450
Ram speed/(mm·s ⁻¹)	5
Friction coefficient of container/billet interface	0.3
Friction coefficient between billet and die	0.3
Total number of elements	20 000
Minimum size of element/mm	1
Mesh density type	Relative
Heat transfer coefficient between tooling and billet/(N·°C ⁻¹ ·s ⁻¹ ·mm ⁻¹)	11
Heat transfer coefficient between tooling/billet and air/(N·°C ⁻¹ ·s ⁻¹ ·mm ⁻¹)	0.02
Relative interference depth/mm	0.7

4 Experimental

The new die installed to Gleeble1500D thermo-mechanical simulator which includes initial extrusion and subsequently shear forming was used in simulation for physical modeling. Fig.5 illustrates the ES die and assemblies. The die parts include two supports, extrusion ram, container and ES forming zone. The transfer corner between compression zone and shear forming zone is 90°. Other structure parameters are the same as those listed in Table 3. The material to manufacture the ES die is H13. Container and ES forming zone are manufactured into a whole. Fig.6 shows the real manufactured object for supports, ES die and extrusion ram. ES die was thread connected with left support and extrusion ram was connected with right support.

Before extrusion, the billets were machined to a diameter of 6 mm. Physical simulations for extrusion

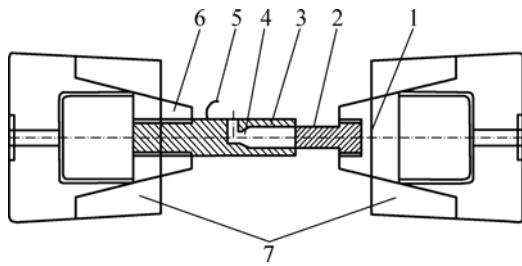


Fig.5 Illustration of ES die and assemblies (1—Right support; 2—Extrusion ram; 3—Container; 4—ES forming zone; 5—Thermocouple; 6—Left support; 7—Fixtures of simulator)

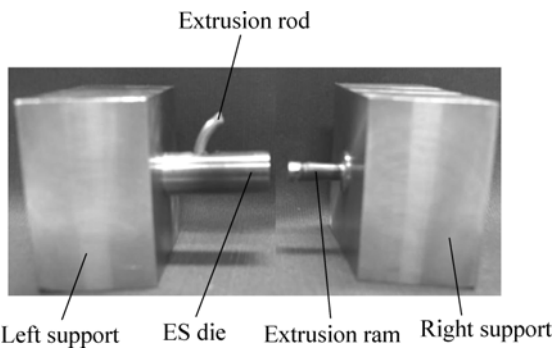


Fig.6 Manufactured ES die and assemblies used on Gleeble1500D thermal simulation equipment

experiments were made by employing Gleeble1500D thermo-mechanical simulator. The steps of installation of experimental equipments and experimental process are as follows. 1) ES die was thread connected with left support, and extrusion ram with right support. 2) The fitted ES die was installed in left fixture of the thermal simulator; and the assembled extrusion ram was fixed in right holder of the thermal simulator. 3) Thermocouple thread was joined to the surface of ES die by welding. 4) The as-extruded AZ31 billet was put into the container; and the assembled extrusion ram was touched with the container by pressure started up with fluid drive for Gleeble1500D. 5) Programming was made and checked carefully in computer of thermal simulator including heating process and extrusion process. The billet and ES die were heated up to 350 °C and then extrusion was started immediately. 6) The programming was executed. The components of ES die and billet were heated for about 10 min and then extruded. Ram speed was 5 mm/s during experimental verification. 7) When extrusion stroke was reached, the programming was stopped and the extrusion rod was taken out.

Immediately after the ES forming, the specimens were water quenched in order to fix the metallurgical structure. The deformed specimens and the unreformed one were then analyzed by means of polarized optical microscopy after an electrolytic etching in a

Barker’s reagent; finally, the grain size distributions were measured and recorded.

5 Results and discussion

5.1 Simulation

From the postprocessor of the DEFORM-3D, the distributions of the effective strain are illustrated in Figs.7(a) and 7(b) when ram strokes are 2.057 and 7.23 mm, respectively. Fig.7(a) shows the strain distributions at the end of forward extrusion when ram stroke is 2.057 mm. The strain distribution is symmetric along the extrusion axes. Fig.7(b) indicates the strain distributions when ram stroke is 7.230 mm. It can be found that the minimum and maximum strains rise from 0 to 0.036 8 and from 4.17 to 4.29, respectively. At the corner from the forward extrusion zone *E* to shearing forming zone *F*, the strains increase obviously from 1.93 to 3.34 (Fig.7(b)). The strains at the portion without shearing forming are increased and the distribution symmetry is retained. The ES forming would increase the cumulative strain enormously compared with the simple forward extrusion.

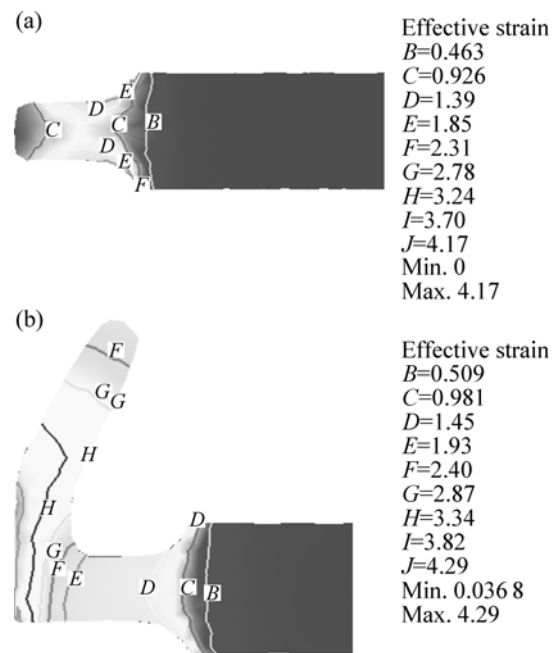


Fig.7 Effective strain distribution from simulation results of ES forming process: (a) Forward extrusion with ram stroke of 2.057 mm; (b) Extrusion including shearing forming with ram stroke of 7.230 mm

The simulation contour for the volume fraction of dynamic recrystallization for ES forming process at ram stroke of 7.230 mm is exhibited in Fig.8. It is discovered that dynamic recrystallization mostly happens at the outside of ES die, and the volume fraction of dynamic recrystallization is more than 10%. During the forward

extrusion, the volume fraction of dynamic recrystallization is very small for the smaller extrusion ratio of 4. The ES forming could refine grains for dynamic recrystallization happens during shearing forming.

5.2 Physical modeling

A laboratory scale testing procedure was defined in order to evaluate the effect of different processing conditions on the evolution of the grain size distribution after deformation of AZ31 alloy provided in standard

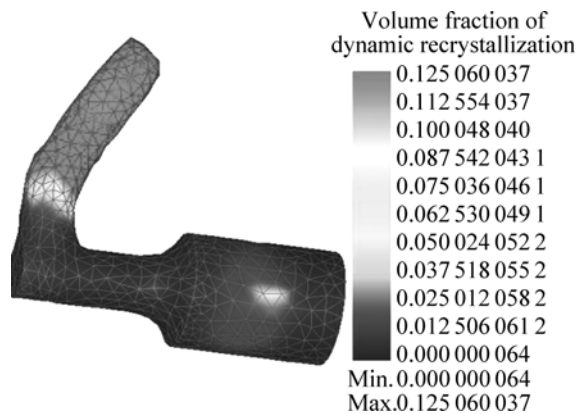


Fig.8 Simulation for volume fraction of dynamic recrystallization at ram stroke of 7.230 mm

industrial homogenization conditions (as-extruded, Mg-3%Al-1%Zn, mass fraction). The examined positions for microstructure have been chosen including cross section and longitudinal directions. Microstructures in the as-received and ES extruded materials for 350 °C were examined following standard metallographic procedures. The polished surface was etched using either a solution of 1% HNO_3 , 24% $\text{C}_2\text{H}_6\text{O}_2$ and 75% H_2O , or 10 mL acetic acid, 4.2 g picric acid and 10 mL H_2O , or 70 mL ethanol. The microstructures were observed by optical microscope (OM).

The as-received (as-extruded) material is characterized by grains with size of 20–50 μm (Fig.9). The microstructures after ES forming along radial direction at 350 °C are shown in Fig.10 and along longitudinal direction in Fig.11. After the process, the grains are equiaxed and distribute more homogeneous than those as-received, with very fine grains of 4–6 μm as well as few coarse grains of larger than 25 μm . A general decrease of grain size is evidenced. This decrease can be explained by the dynamic crystallization effect that reduces the grain dimension without any nucleation of new grains. The initial grain is strongly deformed along one direction, and when the thickness of the grain reaches the subgrain dimension, a new grain is formed.

By comparing the experimental measurements with the FEM-predicted grain size distributions throughout

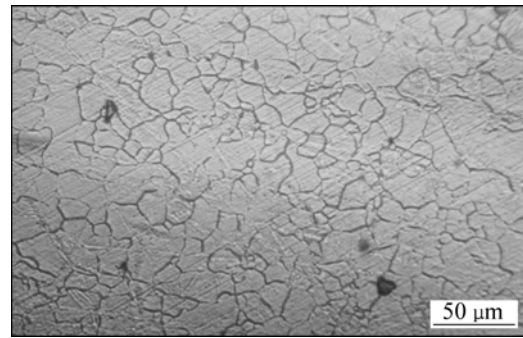


Fig.9 Optical micrograph of as-extruded AZ31 alloy

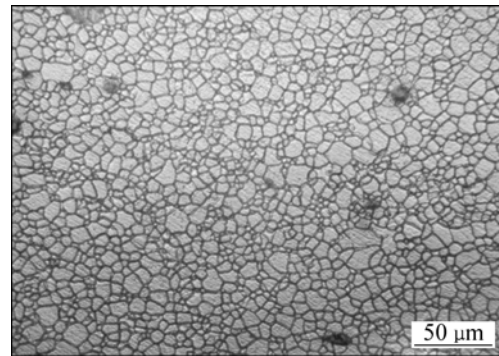


Fig.10 Optical micrograph along radial direction of AZ31 after ES forming

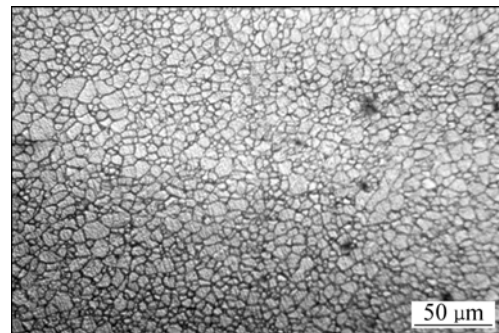


Fig.11 Optical micrograph along longitudinal direction of AZ31 after ES forming

the whole specimen section, there is an interesting agreement between them. From the simulation and experimental results, the ES forming would improve the dynamic recrystallization and refine the grain size effectively.

6 Conclusions

1) A full 3D FEM simulation of as-cast AZ31 magnesium alloy billet subjected to one-pass ES process at 350 °C was carried out successfully. The strain field and the volume fraction of dynamic recrystallization were predicted during ES forming. The simulation results show that the ES forming would cause serve plastic deformation and improve the volume fraction of

dynamic recrystallization during extrusion.

2) The die structures were manufactured and installed to Gleeble1500D thermo-mechanical simulator. ES forming was applied to fabricate AZ31 magnesium alloy rod at temperature of 350 °C and speed of 5 mm/s. The AZ31 magnesium rod has been formed by ES forming.

3) The microstructures of as-received material and the cross section and longitudinal direction for extruded rod were observed. The results validate the ES forming could refine the grains effectively and ES forming is another new serve plastic deformation.

References

- [1] RAGHAVAN S. Computational simulation of the equal channel angular extrusion process [J]. *Scripta Mater*, 2001, 44(1): 91–96.
- [2] LI Yuan-yuan, LIU Ying, NGAI Tungwai Leo. Effects of die angle on microstructures and mechanical properties of AZ31 magnesium alloy processed by equal channel angular pressing [J]. *Trans Nonferrous Met Soc China*, 2004, 14(1): 53–58.
- [3] CHUNG Y H, PARK J W, LEE K H. An analysis of accumulated deformation in the equal channel angular rolling (ECAR) process [J]. *Mater Inter*, 2006, 12(4): 289–293.
- [4] SONG H R, KIM Y S, NAM W J. Mechanical properties of ultrafine grained 5052 Al alloy produced by accumulative roll-bonding and cryogenic rolling [J]. *Metal Mater Inter*, 2006, 12(1): 7–13.
- [5] VALIEV R Z, KRASILNIKOV N A, TSENEV N K. Plastic deformation of alloys with submicron-grained structure [J]. *Mater Sci Eng A*, 1991, 137: 35–40.
- [6] KIM H S, HONG S I, SEO M H. Effects of strain hardenability and strain rate sensitivity on the plastic flow and deformation homogeneity during equal channel angular pressing (ECAP) [J]. *J Mater Res*, 2001, 16: 856–864.
- [7] XING J, SOHDE H, YANG X, MIURA H, SAKAI T. Ultra-fine grain development in magnesium alloy AZ31 during multi-directional forging under decreasing temperature conditions [J]. *Mater Trans*, 2005, 46(20): 1646–1650.
- [8] STAROSELSKY A, ANAND L. A constitutive model for HCP materials deforming by slip and twinning: Application to magnesium alloy AZ31B [J]. *International Journal of Plasticity*, 2003, 19(10): 1843–1864.
- [9] LUIS PÉREZ C J, LURI R. Study of the ECAE process by the upper bound method considering the correct die design [J]. *Mechanics of Materials*, 2008, 40: 617–628.
- [10] CHUNG S W, SOMEKAWA H, KINOSHITA T, KIM W, HIGASHI K. The non-uniform behavior during ECAE process by 3-D FVM simulation [J]. *Scripta Mater*, 2004, 50: 1079–1083.
- [11] JIANG Hong, FAN Zhi-guo, XIE Chao-ying. 3D finite element simulation of deformation behavior of CP-Ti and working load during multi-pass equal channel angular extrusion [J]. *Mater Sci Eng A*, 2007, 485: 409–414.
- [12] VALIEV R Z, ISAMGALIEV R K, ALEXANDROV I V. Bulk nanostructured materials from severe plastic deformation [J]. *Prog Mater Sci*, 2000, 45: 103–189.
- [13] ZHERNAKOV V S, LATYSH V V, ZHARIKOV A I, VALIEV R Z. The developing of nanostructure SPD Ti for structural use [J]. *Scripta Mater*, 2001, 44: 1771–1774.
- [14] WALDE T, RIEDEL H. Modeling texture evolution during hot rolling of magnesium alloy AZ31 [J]. *Mater Sci Eng A*, 2007, 443: 277–284.
- [15] MATSUYAMA K, MIYAHARA Y, HORITA Z, LANGDON T G. Developing superplasticity in a magnesium alloy through a combination of extrusion and ECAP [J]. *Acta Materialia*, 2003, 51: 3073–3084.
- [16] MATSUBARA K, MIYAHARA Y, HORITA Z, LANGDON T G. Achieving enhanced ductility in a dilute magnesium alloy through severe plastic deformation [J]. *Metallurgical and Materials Transactions A*, 2004, 35A: 1734–1744.

(Edited by YANG Bing)